

Oligonol promotes anti-aging pathways *via* modulation of SIRT1-AMPK-Autophagy Pathway

Seul-Ki Park¹, Rak-Kyun Seong¹, Ji-Ae Kim¹, Seok-Jun Son², Younghoon Kim², Takako Yokozawa³ and Ok Sarah Shin^{1,4§}

¹Department of Biomedical Sciences, College of Medicine, Korea University, 145 Anam-ro, Seongbuk-gu, Seoul 02841, Korea

²BK21 Plus Graduate Program, Department of Animal Science and Institute of Rare Earth for Biological Application, Chonbuk National University, Jeonju 54896, Korea

³Institute of Natural Medicine, University of Toyama, Toyama, Japan

⁴Department of Microbiology, College of Medicine, Korea University, Seoul 02841, Korea

BACKGROUND/OBJECTIVES: Oligonol, mainly found in lychee fruit, is an antioxidant polyphenolic compound which has been shown to have anti-inflammatory and anti-cancer properties. The detailed mechanisms by which oligonol may act as an anti-aging molecule have not been determined.

MATERIALS/METHODS: In this study, we evaluated the ability of oligonol to modulate sirtuin (SIRT) expression in human lung epithelial (A549) cells. Oligonol was added to A549 cells and reactive oxygen species production, mitochondrial superoxide formation, and p21 protein levels were measured. Signaling pathways activated upon oligonol treatment were also determined by western blotting. Furthermore, the anti-aging effect of oligonol was evaluated *ex vivo* in mouse splenocytes and *in vivo* in *Caenorhabditis elegans*.

RESULTS: Oligonol specifically induced the expression of SIRT1, whose activity is linked to gene expression, metabolic control, and healthy aging. In response to influenza virus infection of A549 cells, oligonol treatment significantly up-regulated SIRT1 expression and down-regulated viral hemagglutinin expression. Oligonol treatment also resulted in the activation of autophagy pathways and the phosphorylation of AMP-activated protein kinase (AMPK). Furthermore, oligonol-treated spleen lymphocytes from old mice showed increased cell proliferation, and mRNA levels of SIRT1 in the lungs of old mice were significantly lower than those in the lungs of young mice. Additionally, *in vivo* lethality assay revealed that oligonol extended the lifespan of *C. elegans* infected with lethal *Vibrio cholerae*.

CONCLUSIONS: These data demonstrated that oligonol may act as an anti-aging molecule by modulating SIRT1/autophagy/AMPK pathways.

Nutrition Research and Practice 2016;10(1):3-10; doi:10.4162/nrp.2016.10.1.3; pISSN 1976-1457 eISSN 2005-6168

Keywords: Oligonol, SIRT1, senescence, aging

INTRODUCTION

Oligonol, a polyphenolic compound derived from grape seed or lychee fruit, is composed of catechin-type monomers and proanthocyanidin oligomers [1]. *In vivo* studies in animal models and human studies have indicated that oligonol has antioxidant and anti-inflammatory activities, indicating that it could serve as a potential candidate for the treatment and prevention of cancer, type-2 diabetes, inflammatory, and metabolic diseases [2-5]. Recent studies have suggested that the antioxidant role of oligonol may be important for prevention of many diseases and we sought to determine whether the effects of oligonol were directly or indirectly associated with the activation of sirtuin and its targets.

Sirtuins are NAD⁺-dependent protein deacetylases that regulate metabolism and aging and these enzymes have been

shown to mediate the lifespan-extending effects of caloric restriction [6-8]. Resveratrol, a polyphenolic compound found in wine and grapes, is a sirtuin-stimulating compound. Resveratrol has been found to increase the activation of the yeast *Sir2* gene and mammalian SIRT1 gene [9] and it was recently shown that SIRT1 activation alleviated metabolic diseases in mice [10]. Because of SIRT1's role in aging, metabolism, and age-related diseases, small molecules or drugs targeting sirtuins have been implicated in the control of the biochemical, epigenetic, and cellular processes of aging [6].

Recent studies indicate that one of the major roles of the SIRT1-activated pathways is in regulating autophagy [11] and AMP-activated kinase (AMPK), the central energy sensor in the cell [12]. The responsiveness of AMPK signaling attenuates as aging increases, and this loss of sensitivity to cellular stress impairs metabolic regulation, increases oxidative stress, and

This work was supported by a grant from Korea University and Cooperative Research Program for Agriculture Science & Technology Development, Rural Development Administration, Republic of Korea (Project No. PJ010882).

§ Corresponding Author: Ok Sarah Shin, Tel. 82-2-2626-3280 Fax. 82-2-2626-1962 Email. oshin@korea.ac.kr

Received: May 18, 2015, Revised: August 5, 2015, Accepted: August 26, 2015

This is an Open Access article distributed under the terms of the Creative Commons Attribution Non-Commercial License (<http://creativecommons.org/licenses/by-nc/3.0/>) which permits unrestricted non-commercial use, distribution, and reproduction in any medium, provided the original work is properly cited.

reduces autophagic clearance [12]. These age-related changes activate innate immunity, triggering low-grade inflammation and metabolic disorders. Autophagy, a highly orchestrated intracellular degradation process, has emerged as a potential anti-aging mechanism and genetic inhibition of autophagy induces degenerative changes in mammalian tissues that resemble those associated with aging [13].

We wanted to characterize the effect of oligonol on sirtuin expression and downstream signaling pathways using A549 human lung epithelial cells *in vitro* and *C. elegans in vivo*. Our results demonstrated that this antioxidant induced AMPK/autophagy signaling pathways. We also showed that oligonol treatment increased T cell proliferation in old mice and increased the resistance of *C. elegans* to *Vibrio cholerae* infection. Taken together, these data suggested a potential delaying effect of oligonol on cellular senescence and aging.

MATERIALS AND METHODS

Reagents and cell culture

Human lung epithelial cells (A549) were obtained from the American Type Culture Collection (ATCC, Manassas, VA, USA). A549 cells were cultured in RPMI-1640 medium (Thermo Scientific, Waltham, MA, USA) supplemented with 10% (v/v) fetal bovine serum (FBS), 100 U/mL penicillin, and 100 µg/mL streptomycin, and maintained at 37°C with 5% CO₂ in a humidified atmosphere. Oligonol was prepared as described previously [14] and dissolved in dimethyl sulfoxide (DMSO) to a final concentration of 10 mg/mL.

Reactive oxygen species (ROS) assay

Cells were treated with 10 µg/mL oligonol. After 24 h, the cells were washed twice with phosphate-buffered saline (PBS) and stained with 10-µM dichlorofluorescein diacetate (DCF-DA) (Sigma, St. Louis, MO, USA) in PBS for 30 min in the dark. Cells were then washed twice with PBS and extracted with PBS for 10 min at 37°C. Fluorescence was recorded using a spectrofluorometer (VICTOR3, Perkin-Elmer, Waltham, MA, USA) with an excitation wavelength of 490nm and an emission wavelength of 525nm.

Mitochondrial superoxide measurement

Mitochondrial superoxide levels were determined by staining with MitoSOX Red (Invitrogen, Carlsbad, CA, USA). Oligonol-treated cells were incubated with 2.5-µM MitoSOX Red at 37°C for 15 min. The coverslips were mounted onto glass slides using mounting media containing 4,6-diamidino-2-phenylindole (Sigma) prior to examination using a confocal microscope (LSM700, Zeiss, Jena, Germany).

Reverse transcription PCR (RT-PCR) and quantitative real-time PCR (qRT-PCR)

RNA isolation and cDNA synthesis were performed as described previously [15]. Briefly, total RNA (1 µg) was isolated with Trizol reagent (Invitrogen) and reverse transcribed using the RT system (Promega, Madison, WI, USA) for 1 h at 42°C. For RT-PCR, the thermal cycling conditions consisted of 40 cycles of denaturation at 95°C for 30 s, annealing at 60°C for

Table 1. Primers used in the quantitative real-time polymerase chain reaction study

Target mRNA	Forward 5' → 3'	Reverse 5' → 3'
hSIRT1	TAGCCTTGTCAGATAAGGAAGGA	ACAGCTTCACAGTCAACTTTGT
hSIRT2	TGCGGAACTTATTCTCCAGAGA	GAGAGCGAAAGTCGGGGAT
hSIRT3	ACCCAGTGGCATTCCAGAC	GGCTTGGGGTTGTGAAAGAAG
hSIRT4	AGCCTCCATTGGGTTATTTGTG	TCTGGTATCCCCGATTCGGT
hSIRT5	GCCATAGCCGAGTGTGAGAC	CAACTCCACAAGAGGTACATCG
hSIRT6	CCCACGGAGTCTGGACCAT	CTCTGCCAGTTTGTCCCTG
hSIRT7	GACCTGGTAACGGAGCTGC	CGACCAAGTATTTGGCGTTCC
hSOD1	TGGAAGTCGTTTGGCTTGT	TGGAAGTCGTTTGGCTTGT
hSOD2	GGGATGCCTTT TAG TCC TAT TC	TATAGAAAGCCG AGT GTT TCCC
hβ-actin	CCACACCTTCTACAATGAGCTGCG	CGGAGTCCATCACGATCCA
mSIRT1	TAGATACCTTGGAGCAGGTTG	CAGTAATTTCTGAAAGCTTTACA GGG
mGAPDH	CAAGGAGTAAGAAACCCTGGACC	CGAGTTGGATAGGGCCTCT
Influenza HA	TTGCTAAAACCCGGAGACAC	CCTGACGTATTTTGGGCACT

30 s, and extension at 72°C for 30 s. For qRT-PCR, Power SYBR Green Master Mix (Applied Biosystems, Foster City, CA, USA) was used to measure human and mouse mRNA expression. Primer sequences are shown in Table 1. The PCR included one incubation at 95°C for 15 min, followed by 40 cycles of 30 s at 95°C and 1 min at 60°C. β-actin or Glyceraldehyde 3-phosphate dehydrogenase (GAPDH) mRNA was used to normalize the data. Expression was calculated using the ΔCt method, where the amount of target, normalized to an endogenous reference mRNA and relative to a calibrator, is given by 2^{-ΔΔCt}, where Ct is the cycle number of the detection threshold.

Western blotting

Cellular lysates were prepared with lysis buffer (Cell Signaling, Beverly, MA, USA) and then separated by sodium dodecyl sulfate-polyacrylamide gel electrophoresis (SDS-PAGE) on 10-12% polyacrylamide gels and transferred to polyvinylidene difluoride membranes. The membranes were incubated in blocking buffer (TBS/T; 5% non-fat milk in 0.2 M Tris, 1.36 M NaCl, 0.1% Tween 20) for 1 h at room temperature, and then washed three times for 5 min each with 15 mL of TBS/T. Membranes were incubated overnight with the primary antibodies at 4°C. Antibodies against SIRT1, p21, Microtubule-associated protein 1A/1B-light chain 3 (LC3) LC3A/B, p62, phospho-AMPK, total AMPK, and Phospho-Acetyl-CoA Carboxylase (Ser79) were purchased from Cell Signaling. An anti-GAPDH antibody was purchased from Sigma. The membranes were washed three times with TBS/T and then incubated with horseradish peroxidase-conjugated anti-rabbit IgG secondary antibody for 1 h at 25°C. After washing three times with TBS/T, the membranes were incubated with PierceTM ECL Western Blotting Substrate (Invitrogen) and exposed to film.

Enzyme-linked immunosorbent assay (ELISA)

Supernatants were collected after 24-h exposure to oligonol and stored at -80°C until assay. Interleukin-8 (IL-8) protein levels were determined by ELISA according to the manufacturer's instructions (Biolegend, San Diego, CA, USA). Absorbance was detected with a microplate reader at 450nm.

Lymphocyte proliferation studies using mouse splenocytes

This animal study was approved by the Korea University

School of Medicine Institutional Animal Care and Use Committee (KUIACUC-20141105-3). Splens were collected from young (3-4 months) and old (18-24 months) C57BL/6 mice under aseptic conditions in HBSS. Splenocytes were collected by passing spleen tissue through a fine steel mesh to obtain a homogeneous cell suspension; the erythrocytes were lysed with ammonium chloride (0.8%, w/v). After centrifugation (380 × g at 4°C for 10 min), the pelleted cells were washed three times with PBS and resuspended in complete medium [RPMI 1640 supplemented with 12 mM HEPES (pH 7.1), 0.05 mM 2-mercaptoethanol, 100 U/mL penicillin, 100 µg/mL streptomycin, and 10% FBS]. The spleen cell suspension (2 × 10⁵ cells/mL) was pipetted into 96-well plates (200 µL/well) and cultured at 37°C for 72 h in a humid atmosphere containing 5% CO₂ in the presence of recombinant protein IL-2. After 72 h, (4, 5-dimethylthiazolyl-2)-2,5-diphenyltetrazolium bromide (MTT) solution was added to each well and the plates were incubated for 4 h. Then, DMSO was added for 15 min prior to reading absorbance. The absorbance was evaluated in a microplate reader at 540nm

Mouse lung tissues

Mouse lung tissues were obtained from the Aging Tissue Bank (Pusan, Korea). Senescence marker protein (SMP)30^{+/+} and SMP30^{-/-} mice were described previously [16]. Total RNA was purified using the RNeasy Mini Kit (Qiagen), according to the manufacturer's recommended protocol.

Influenza virus infection model

Human influenza virus A/Puerto-Rico/8/34 (H1N1) PR8 virus was kindly provided by Dr. Man Sung Park (Department of Microbiology, College of Medicine, Korea University, Korea). Virus infectivity titers of supernatants were determined by plaque assay [17]. Human lung epithelial cells (A549) were seeded on 60-mm dishes and treated with oligonol at a concentration of 10 µg/mL for 2 h followed by PR8 infection at a multiplicity of infection of 0.1 for 1 h. Virus infection was performed in infection media (DMEM containing 2% FBS and 2 µg/mL tosylsulfonyl phenylalanyl chloromethyl ketone (TPCK)) for 1 h at 37°C. Cells were then washed with PBS and cultured in DMEM with 2% FBS for another 24 h. qRT-PCR was performed to determine mRNA expression of influenza hemagglutinin (HA).

Caenorhabditis elegans survival assays

The *C. elegans* fer-15(b26)II; fem-1(hc17) line was selected for liquid assay experiments because it is unable to produce progeny at 25°C [18]. These worms were infected as described previously [19]. Worms were cultured and maintained on nematode growth medium agar containing lawns of *Escherichia coli* OP50. To assess the susceptibility of *C. elegans* to infection by *V. cholerae*, the bacteria were cultured in brain-heart infusion media (BHI) at 37°C. Synchronized young adult/L4 worms were infected on lawns of *V. cholerae* strains for 24 h at 25°C. After washing three times with M9 buffer, worms were transferred into 6-well plates (30 worms per well). Each well contained 2 mL assay medium (20% BHI:80% M9; v/v) supplemented with 1, 10, or 100 µg/mL oligonol. DMSO only was employed as control. The plates were incubated at 25°C and examined for viability at 24-h intervals for 12 days using a Nikon SMZ645

dissecting microscope. Biological replicates of each experiment were conducted.

Statistical analysis

The results were expressed as the mean ± SD. The data were analyzed using Student's *t*-test to determine the significance of the difference between two groups. Statistics were performed using Prism software. A *P*-value < 0.05 was considered statistically significant. Differences in *C. elegans* survival were tested for significance by Kaplan-Meier and log-rank tests (STATA6; STATA, College Station, TX, USA). A two-tailed *P*-value of < 0.05 was considered statistically significant.

RESULTS

Activation of SIRT1, autophagy, and the AMPK pathway in A549 cells exposed to oligonol

To study aging using an *in vitro* model, we used lung epithelial cells (A549) at a high passage number, because aging increases susceptibility to respiratory infections. To determine whether oligonol caused cytotoxicity in A549 cells, various concentrations of oligonol were added to the cells for 24 h prior to MTT assay. Even a high concentration of oligonol (100 µg/mL) did not inhibit the growth of high-passage A549 cells (Fig. 1A). ROS formation was significantly attenuated by oligonol, as shown by the DCF-DA fluorescence (Fig. 1B). We also investigated whether oligonol modulated mitochondrial superoxide formation in A549 cells. Oligonol treatment decreased the numbers of cells with mitochondrial superoxide formation, indicating that it had antioxidant activity (Fig. 1C). Furthermore, oligonol-treated cells produced less pro-inflammatory IL-8 than untreated cells (Fig. 1D).

Sirtuins regulate metabolism and aging, and augment lifespan in some organisms [6]. To estimate the anti-aging effects of oligonol on sirtuin gene expression, A549 cells were treated with oligonol for 2 h. qRT-PCR was performed to investigate sirtuin (SIRT1-7) mRNA expression (Fig. 2A). SIRT 2, 3, 4, 5, and 6 mRNA expression levels were not affected by oligonol, whereas SIRT7 expression was attenuated in cells exposed to oligonol. However, qRT-PCR analysis indicated that SIRT1 mRNA expression was increased by 3-fold in cells exposed to oligonol. We also examined the expression of two mitochondrial antioxidant enzymes, superoxide dismutase (SOD) 1 and 2, and found that SOD2 mRNA levels were also up-regulated by oligonol treatment (Fig. 2B).

Given that oligonol has been shown to have anti-influenza activity [20], and SIRT1 also showed an anti-viral effect [21], we sought to determine whether oligonol modulated SIRT1 expression during influenza virus infection in A549 cells. As previously reported by another group [20], we observed that oligonol treatment of A549 cells prior to influenza virus infection led to a significant reduction in viral replication, resulting in a complete block of the expression of influenza HA in A549 cells. In the present study, influenza infection alone did not induce SIRT1 mRNA expression; however, treatment of influenza-infected cells with oligonol significantly increased SIRT1 mRNA expression by ~15-fold (Fig. 2D). These data suggested the possibility that oligonol-mediated anti-influenza

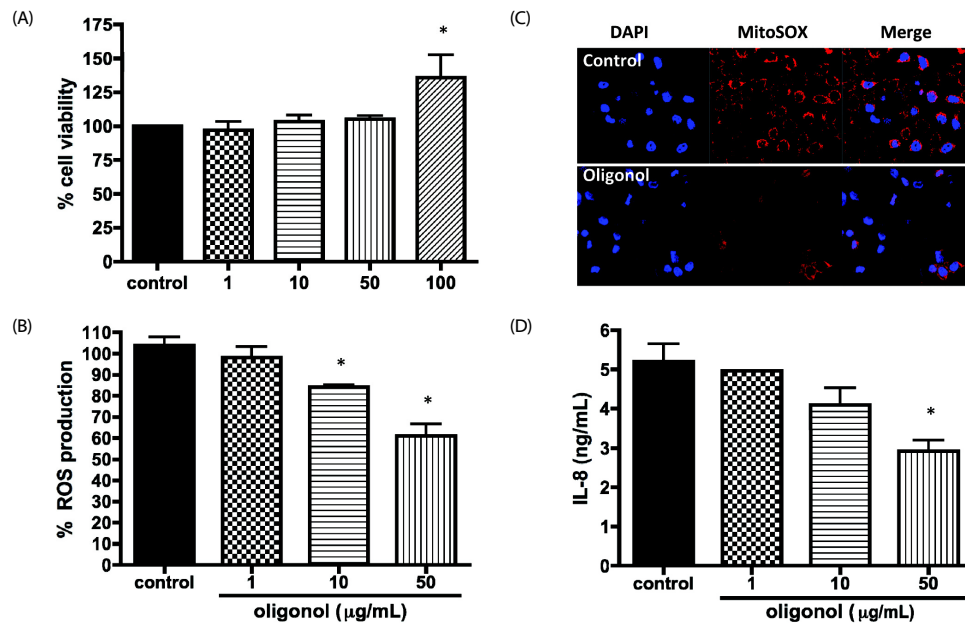


Fig. 1. Oligonol suppressed reactive oxygen species (ROS) production in human lung epithelial cells. (A) A549 cells were treated with oligonol at 1, 10, 50, or 100 $\mu\text{g/mL}$ and cell viability was determined by the MTT assay. Data are shown as the mean \pm SD of three independent experiments. (B) High-passage A549 cells were treated with oligonol at a concentration of 1, 10, or 50 $\mu\text{g/mL}$ for 24 h and the total ROS level was determined using dichlorofluorescein diacetate (DCF-DA). Data are shown as the mean \pm SD of three independent experiments and are presented as the percentage of control (dimethyl sulfoxide [DMSO]-treated). (C) Mitochondrial superoxide production was evaluated by detecting MitoSOX-positive cells using confocal microscopy. (D) Interleukin-8 (IL-8) levels were measured by enzyme-linked immunosorbent assay after oligonol treatment. Data are shown as the mean \pm SD of three independent experiments and are presented as the percentage of control (DMSO-treated). * $P < 0.05$ vs. the DMSO control cells.

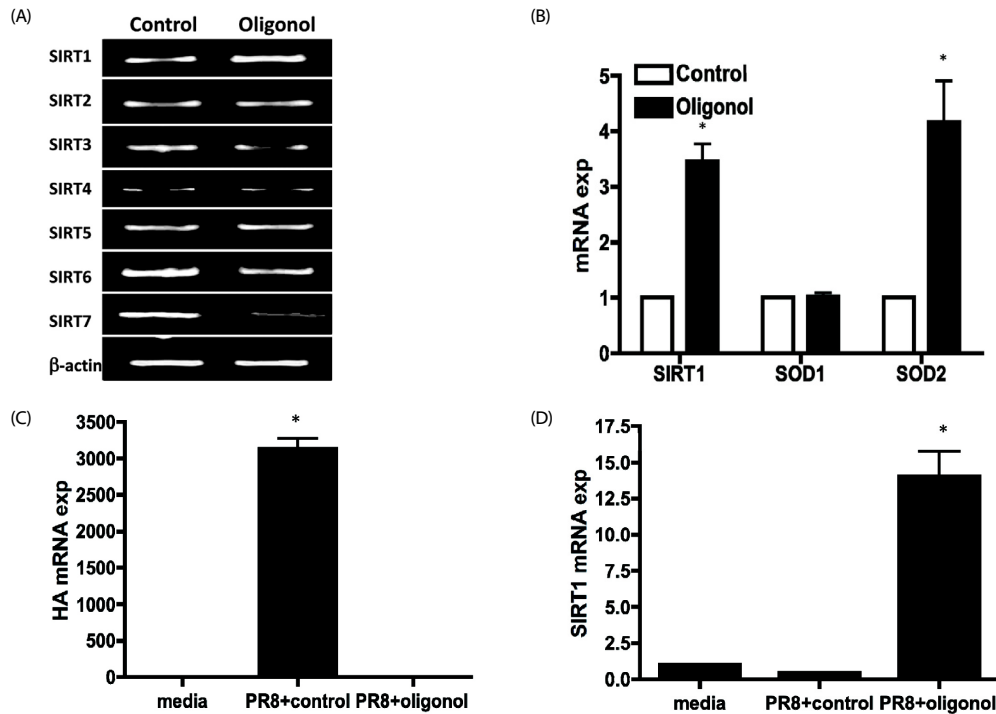


Fig. 2. Oligonol up-regulated sirtuin 1 (SIRT1) expression. (A) High-passage A549 cells were treated with 10 $\mu\text{g/mL}$ oligonol for 2 h, total cellular RNA was isolated, and SIRT1-7 mRNA levels were measured by reverse transcription PCR (RT-PCR). (B) The mRNA levels of SIRT1 were determined by quantitative real-time PCR (qRT-PCR). The value obtained for control (dimethyl sulfoxide [DMSO]-treated) cells was arbitrarily set to 1, and relative expression is shown in the graph. Expression of target genes was normalized to that of β -actin. The qRT-PCR experiments were performed in duplicate and data are shown as the mean \pm SD of three independent experiments. * $P < 0.05$ vs. DMSO control cells. (C) High-passage A549 cells were treated with 10 $\mu\text{g/mL}$ oligonol for 2 h before infection with PR8 influenza virus at a multiplicity of infection of 0.1 and incubation for 24 h prior to RNA isolation. Expression of a major influenza antigen, hemagglutinin (HA) (C) and SIRT1 (D) were measured and normalized to that of β -actin. The qRT-PCR experiments were performed in duplicate and data are shown as the mean \pm SD of three independent experiments.

activity may be associated with its up-regulation of SIRT1 expression.

We used immunofluorescence staining with LC3, a marker protein for autophagy, to assess the effect of oligonol on autophagy in A549 cells. We observed that oligonol induced higher numbers of visible LC3 puncta in A549 cells, as compared with control treated cells (Fig. 3A). Next, we measured the protein levels of LC3-II and p62/SQSTM1, two protein markers of autophagy, using western blotting. Detection of LC3 by immunoblotting or immunofluorescence provides a reliable method to monitor autophagy, whereas the levels of p62/SQSTM1, a ubiquitin- and LC3-binding protein, increase when autophagy is impaired [13]. Oligonol treatment significantly

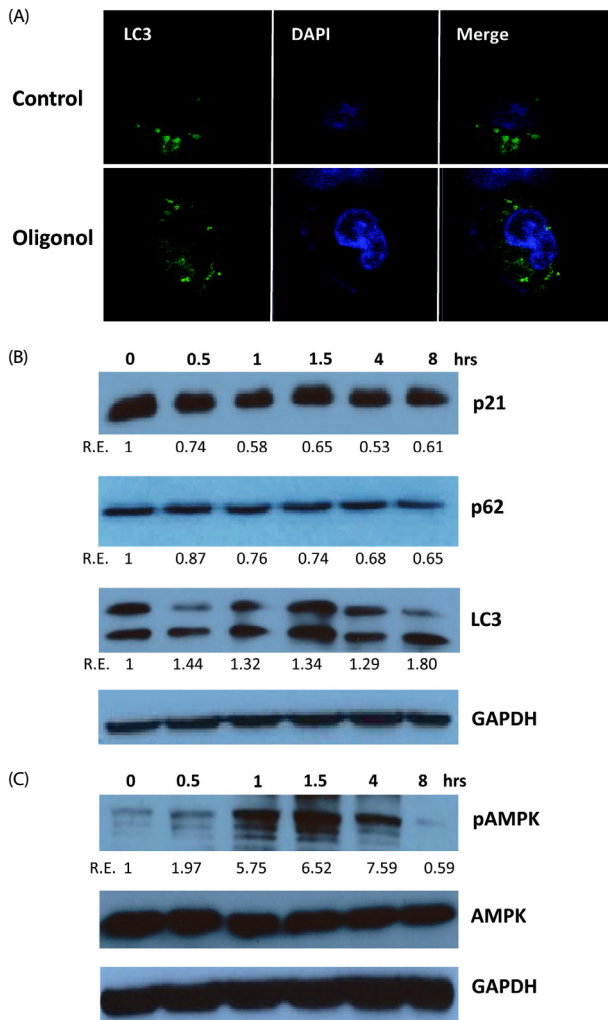


Fig. 3. Oligonol induced the AMP-activated protein kinase (AMPK)/autophagy pathway. (A) For the measurement of autophagy, high-passage A549 cells were treated with control or 10 µg/mL oligonol for 24 h and cells were stained with anti-LC3 antibody. Cells were examined by fluorescence confocal microscopy. Magnification $\times 400$. (B) High-passage cells were treated with 10 µg/mL oligonol for various times (0, 0.5, 1, 1.5, 4, or 8 h) and total cellular lysates were collected for western blotting. Expression of the indicated proteins were determined using the relevant antibodies. Representative images are shown from three independent experiments. (C) Phosphorylation of AMPK was measured using antibodies detecting total AMPK and phospho-AMPK (active form, phosphorylated at Thr172). Protein bands were quantified using densitometry, and the normalized densitometric units were plotted against the relevant treatment (R.E.: Relative Expression).

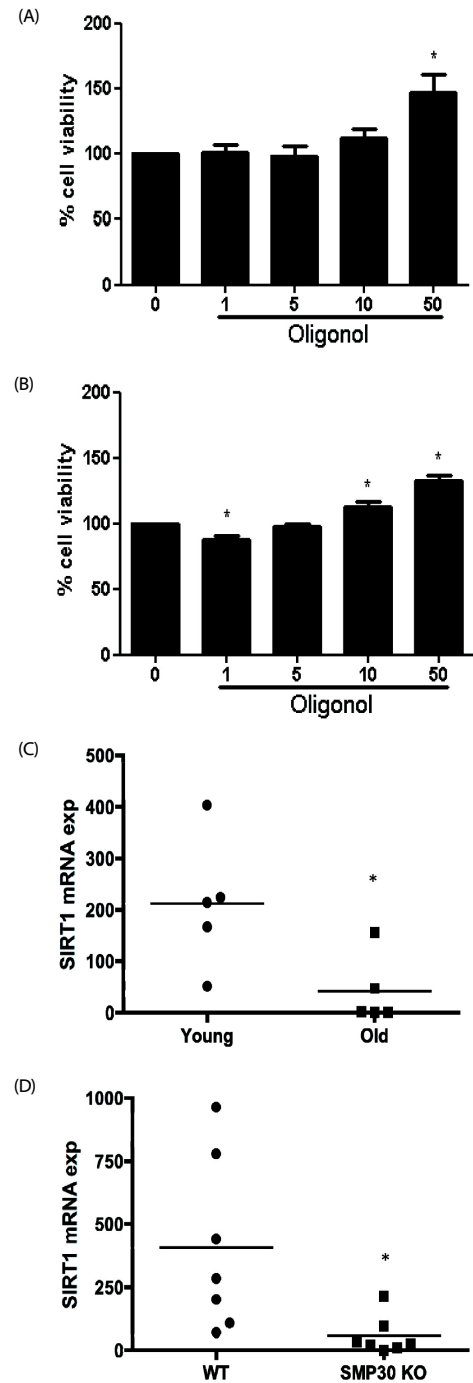


Fig. 4. Oligonol induced splenocyte proliferation in old mice. Splenocytes were obtained from young (3-4 months) (A) and old (18-24 months) (B) C57BL/6 mice. Splenocytes were incubated with interleukin-2 (IL-2) for 48 h and then with various concentrations (1, 5, 10, 50 µg/mL) of oligonol for another 48 h. Colorimetric determination of MTT reduction was made at 540nm and % cell viability is shown in the graph. The assays were performed in duplicate and data are shown as the mean \pm SD of three mice. (C) Lung tissues from young and old mice. (D) Lung tissues from senescence marker protein-30 (SMP30) knock-out (SMP30^{-/-}) and wild-type (SMP30^{+/+}) mice were collected and SIRT1 mRNA levels were examined by quantitative real-time PCR (qRT-PCR). Target gene expression was normalized to that of mouse glyceraldehyde 3-phosphate dehydrogenase (GAPDH). The qRT-PCR experiments were performed in duplicate and each symbol represents the value for an individual mouse. The bar indicates the mean for the study group. * $P < 0.05$ for the comparison with the control group, Kruskal-Wallis test (one-way analysis of variance).

promoted LC3-II levels and reduced p62/SQSTM1 levels in A549 cells (Fig. 3B). In addition, expression of a cellular senescence marker (p21) was reduced by oligonol treatment. We next explored the potential mechanisms underlying oligonol-induced autophagy and examined AMPK, a ubiquitous sensor of cellular energy status, which has been shown to be connected to increased autophagic activity [22]. We found that oligonol increased the phosphorylation of AMPK at early time-points (Fig. 3C).

Oligonol affected splenocyte proliferation in old mice

To investigate the effect of oligonol on the cellular immune response using an *ex vivo* system, we evaluated IL-2-induced splenocyte proliferation in mice using the MTT assay. Splenocytes were isolated from both young (3-4 months) and old (18-24 months) mice and cell viability was measured in the presence or absence of oligonol. The results indicated that whereas oligonol treatment of splenocytes isolated from young mice only induced a significant increase in splenocyte proliferation at a concentration of 50 $\mu\text{g}/\text{mL}$, oligonol levels as low as 1 $\mu\text{g}/\text{mL}$ increased the proliferation of splenocytes from old mice in a concentration-dependent manner, suggesting that oligonol induced cellular proliferation in aged cells (Fig 4A).

It has been suggested that older animals produce less SIRT1 [23]. Hence, we examined the expression of SIRT1 in the lungs of young (3-4 months) and old (18-24 months) mice. Similarly, we also compared the expression of SIRT1 in the lungs of 6-month-old wild-type and SMP-30 knockout mice, which has been suggested to provide a useful model of senescence [24]. SIRT1 mRNA levels were significantly lower in the lungs of the old mice than in those of the young mice (Fig 4B). This suggested that the increased susceptibility of aged animals could be attributed to their lower SIRT1 expression and the subsequent decrease in the expression of other receptors and signaling molecules in the lungs. On the other hand, the mean expression levels of inflammatory molecules, such as IP-10,

RANTES, MCP-1, and TNF- α transcripts, were significantly higher in old mice than in young mice (data not shown).

Oligonol treatment promoted survival of *C. elegans* infected with *V. cholerae*

C. elegans is an established invertebrate host model for investigating the molecular mechanisms of aging and longevity [25]. Moreover, it can be used for identifying and assessing the virulence of several human pathogens, including *V. cholerae* [26, 27]. We tested the ability of oligonol to promote longevity and induce anti-microbial activity *in vivo* using *C. elegans* liquid-killing assays. Consistent with previous results, exposure of control *C. elegans* to *V. cholerae* infection led to their death within ~8 days. Surprisingly, oligonol treatment (100 $\mu\text{g}/\text{mL}$) increased the lifespan of *V. cholerae*-infected worms significantly ($P = 0.0001$, as compared with DMSO control worms) (Fig. 5). These data suggested that oligonol increased *C. elegans* survival by modulating the *in vivo* host defense against enteric pathogens.

DISCUSSION

Oligonol has been suggested to have a beneficial effect on inflammatory diseases or cancer [2,3,20,28-30]. This oligonol-mediated protection could be due to its antioxidant activity. In this study, we examined the role of oligonol as an anti-aging molecule. Our studies demonstrated that oligonol inhibited the production of ROS and mitochondrial superoxide in human lung epithelial cells. Oligonol also significantly up-regulated SIRT1 gene expression and the autophagic AMPK pathway in a time-dependent manner. Furthermore, oligonol treatment increased the proliferation of splenocytes from old mice and prolonged *C. elegans* lifespan by enhancing the host defense response against a microbial infection. These and other results are consistent with the suggestion that oligonol had anti-aging effects.

Mounting evidence points to the beneficial effects of plant-based polyphenolic compounds in aging-associated inflammatory disorders. We found that oligonol induced phosphorylation of proteins in the AMPK signaling pathway, as well as inducing autophagy. AMPK, a member of the AMPK protein kinase family, is a central energy sensor and metabolic switch found in all eukaryotes [12]. Recent reports have indicated that AMPK mediates the acute autophagic response by interacting with ULK1 [22], implying an essential role for AMPK in the autophagy process.

Excessive accumulation of ROS and oxidative damage has been linked to multiple diseases, including neurodegenerative diseases, diabetes, cancer, and premature aging [31,32]. There are multiple sources of ROS in the cell, and mitochondria are a major site of ROS production. It was recently shown that increased mitochondrial ROS production was directly associated with increased production of pro-inflammatory cytokines and susceptibility to pathological conditions as diverse as malignancies, autoimmune diseases, and cardiovascular diseases [33]. Thus, we examined the antioxidant effect of oligonol by measuring total ROS in high-passage A549 cells, as well as mitochondrial superoxide production. Increased ROS production is closely linked to mitochondrial dysfunction and we

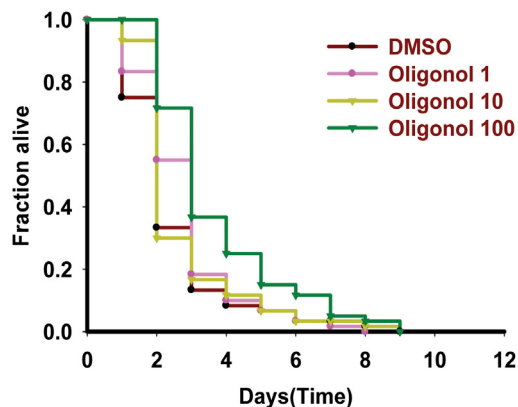


Fig. 5. Oligonol delayed lethality during *Vibrio cholerae* infection in *Caenorhabditis elegans*. Lethality analysis was performed in *C. elegans* fer-15(b26)ll; fem-1(hc17) that were fed with *V. cholerae*. Worms were treated with medium supplemented with 1, 10, or 100 $\mu\text{g}/\text{mL}$ of oligonol in 6-well plates (30 worms per well). Controls were maintained in medium supplemented with dimethyl sulfoxide (DMSO). Assay plates were kept at 25°C and scored for survivors at 24-h intervals. Data were plotted using the Kaplan-Meier method and survival curves were compared using the log-rank test. P values for oligonol: 1 $\mu\text{g}/\text{mL} = 0.0501$, 10 $\mu\text{g}/\text{mL} = 0.3570$, and 100 $\mu\text{g}/\text{mL} = 0.0001$.

therefore measured superoxide production from mitochondria specifically by MitoSOX staining [34]. DCF-DA revealed lower ROS levels in oligonol-treated cells and there was a specific inhibition of mitochondrial superoxide formation (Fig. 1C). Thus, targeting mitochondrial ROS can be driven by the antioxidant effects of oligonol and this could directly contribute to delaying cellular senescence.

The mammalian sirtuins (SIRT1-7) are a conserved family of NAD⁺-dependent deacetylases and ADP-ribosyltransferases involved in numerous fundamental cellular processes, including gene silencing, DNA repair, and metabolic regulation [8]. Recent human genetic studies also supported a role for SIRT1 in maintaining human health status with age [35]. In 2003, a screen for small molecule activators of SIRT1 identified 21 different SIRT1-activating molecules, the most potent of which was resveratrol [7]. The effects of resveratrol on aging and disease have been extensively studied to date and this compound has been found to increase lifespan in *Saccharomyces cerevisiae*, *C. elegans*, and *Drosophila melanogaster* in a sirtuin-dependent manner, although the lifespan extension in yeast and flies, and the Sir2-dependence in worms, have subsequently been challenged [36]. Sirtuins are attractive drug targets and the compounds and mechanisms regulating their activity have been studied intensely [6]. Given that oligonol treatment promotes survival in *C. elegans* during *V. cholerae* infection and up-regulated proliferation of splenocytes isolated from old mice, it may be worthwhile to carry out further studies of the benefits of oligonol treatment in other animal models of aging-mediated disease.

In addition to exploring the efficacy of oligonol as a potential treatment for inflammation, viral diseases, and cancer, recent studies have addressed the role of oligonol in metabolic control. For example, oligonol inhibited adipogenesis *via* Akt-mTOR inhibition in a cellular model [37], whereas oligonol treatment of diabetes-prone mice attenuated diabetes-induced renal damage [38]. Correlating well with previous data, our results also suggested a metabolic control effect of oligonol, which activated AMPK. Interestingly, SIRT1 and AMPK have been shown to play many similar roles, including their ability to respond to stress and nutrient status, induce mitochondrial biogenesis, regulate glucose homeostasis, and control the activity of important transcriptional regulators such as Peroxisome proliferator-activated receptor-gamma coactivator 1 alpha (PGC-1 α), FoxO, and p300 [39] AMPK has been shown to activate SIRT1, likely indirectly *via* an increase in the cellular NAD⁺ level [40]. Given that AMPK has been shown to mediate the antioxidant effects of resveratrol through regulation of the transcription factor, FoxO1, it is highly possible that the antioxidant effect of oligonol depends on AMPK pathway activation.

The present study generated data indicating that oligonol treatment may exert an antioxidant effect in high-passage cells, potentially *via* the activation of the SIRT1/AMPK/autophagy pathway (Fig. 6). Our data showing that oligonol extended the lifespan of *C. elegans* infected with *V. cholerae* suggest an important role for oligonol as an anti-aging compound *in vivo*. One limitation of this study was the lack of an aged *in vivo* model to explore the long-term effects of oligonol (as a dietary supplement) on the aging process. Further studies including

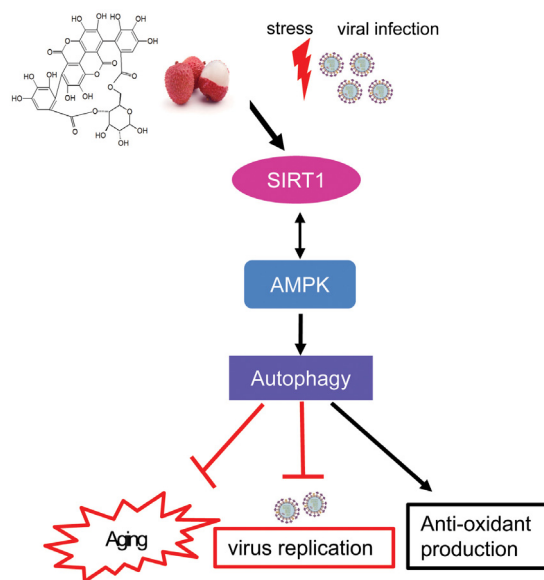


Fig. 6. Schematic representation of oligonol-mediated activation of sirtuin 1 (SIRT1)-AMP-activated protein kinase (AMPK)-autophagy pathways. In the presence of oxidative stress or viral infection, oligonol treatment can enhance SIRT1 expression and downstream signaling pathways, leading to activation of autophagy and AMPK pathways. As a result, this may contribute to up-regulation of antioxidant formation and inhibition of viral replication.

oral administration of oligonol in aged animal models will provide an insight into the possible development of oligonol in preventing age-related disorders. Collectively, our data suggested that SIRT1-inducing oligonol could be introduced as a potential supplement to promote healthy aging.

ACKNOWLEDGEMENTS

We thank the Aging Tissue Bank for providing research materials for this study and Dr. Man-Sung Park (Korea University School of Medicine) for providing the PR8 influenza virus.

REFERENCES

- Fujii H, Sun B, Nishioka H, Hirose A, Aruoma OI. Evaluation of the safety and toxicity of the oligomerized polyphenol Oligonol. *Food Chem Toxicol* 2007;45:378-87.
- Tomobe K, Fujii H, Sun B, Nishioka H, Aruoma OI. Modulation of infection-induced inflammation and locomotive deficit and longevity in senescence-accelerated mice-prone (SAMP8) model by the oligomerized polyphenol Oligonol. *Biomed Pharmacother* 2007; 61:427-34.
- Kundu JK, Hwang DM, Lee JC, Chang EJ, Shin YK, Fujii H, Sun B, Surh YJ. Inhibitory effects of oligonol on phorbol ester-induced tumor promotion and COX-2 expression in mouse skin: NF-kappaB and C/EBP as potential targets. *Cancer Lett* 2009;273:86-97.
- Lee SJ, Chung IM, Kim MY, Park KD, Park WH, Moon HI. Inhibition of lung metastasis in mice by oligonol. *Phytother Res* 2009;23: 1043-6.
- Park CH, Noh JS, Fujii H, Roh SS, Song YO, Choi JS, Chung HY, Yokozawa T. Oligonol, a low-molecular-weight polyphenol derived from lychee fruit, attenuates gluco-lipotoxicity-mediated renal disorder

- in type 2 diabetic db/db mice. *Drug Discov Ther* 2015;9:13-22.
6. Guarente L. Sirtuins, aging, and metabolism. *Cold Spring Harb Symp Quant Biol* 2011;76:81-90.
 7. Howitz KT, Bitterman KJ, Cohen HY, Lamming DW, Lavu S, Wood JG, Zipkin RE, Chung P, Kisielewski A, Zhang LL, Scherer B, Sinclair DA. Small molecule activators of sirtuins extend *Saccharomyces cerevisiae* lifespan. *Nature* 2003;425:191-6.
 8. Haigis MC, Sinclair DA. Mammalian sirtuins: biological insights and disease relevance. *Annu Rev Pathol* 2010;5:253-95.
 9. Korkina LG, Pastore S, Dellambra E, De Luca C. New molecular and cellular targets for chemoprevention and treatment of skin tumors by plant polyphenols: a critical review. *Curr Med Chem* 2013;20:852-68.
 10. Wu Y, Li X, Zhu JX, Xie W, Le W, Fan Z, Jankovic J, Pan T. Resveratrol-activated AMPK/SIRT1/autophagy in cellular models of Parkinson's disease. *Neurosignals* 2011;19:163-74.
 11. Lee IH, Cao L, Mostoslavsky R, Lombard DB, Liu J, Bruns NE, Tsokos M, Alt FW, Finkel T. A role for the NAD-dependent deacetylase SIRT1 in the regulation of autophagy. *Proc Natl Acad Sci U S A* 2008;105:3374-9.
 12. Salminen A, Kaarniranta K. AMP-activated protein kinase (AMPK) controls the aging process via an integrated signaling network. *Ageing Res Rev* 2012;11:230-41.
 13. Rubinsztein DC, Mariño G, Kroemer G. Autophagy and aging. *Cell* 2011;146:682-95.
 14. Fujii H, Nakagawa T, Nishioka H, Sato E, Hirose A, Ueno Y, Sun B, Yokozawa T, Nonaka G. Preparation, characterization, and antioxidative effects of oligomeric proanthocyanidin-L-cysteine complexes. *J Agric Food Chem* 2007;55:1525-31.
 15. Shin OS, Yanagihara R, Song JW. Distinct innate immune responses in human macrophages and endothelial cells infected with shrew-borne hantaviruses. *Virology* 2012;434:43-9.
 16. Jung KJ, Lee EK, Kim SJ, Song CW, Maruyama N, Ishigami A, Kim ND, Im DS, Yu BP, Chung HY. Anti-inflammatory activity of SMP30 modulates NF-kappaB through protein tyrosine kinase/phosphatase balance. *J Mol Med (Berl)* 2015;93:343-56.
 17. Kim JI, Park S, Lee I, Lee S, Shin S, Won Y, Hwang MW, Bae JY, Heo J, Hyun HE, Jun H, Lim SS, Park MS. GFP-expressing influenza A virus for evaluation of the efficacy of antiviral agents. *J Microbiol* 2012;50:359-62.
 18. Kim Y, Mylonakis E. *Caenorhabditis elegans* immune conditioning with the probiotic bacterium *Lactobacillus acidophilus* strain NCFM enhances gram-positive immune responses. *Infect Immun* 2012;80:2500-8.
 19. Kim HI, Kim JA, Choi EJ, Harris JB, Jeong SY, Son SJ, Kim Y, Shin OS. In vitro and in vivo antimicrobial efficacy of natural plant-derived compounds against *Vibrio cholerae* of O1 El Tor Inaba serotype. *Biosci Biotechnol Biochem* 2015;79:475-83.
 20. Gangehei L, Ali M, Zhang W, Chen Z, Wakame K, Haidari M. Oligonol a low molecular weight polyphenol of lychee fruit extract inhibits proliferation of influenza virus by blocking reactive oxygen species-dependent ERK phosphorylation. *Phytomedicine* 2010;17:1047-56.
 21. Koyuncu E, Budayeva HG, Miteva YV, Ricci DP, Silhavy TJ, Shenk T, Cristea IM. Sirtuins are evolutionarily conserved viral restriction factors. *MBio* 2014;5:pil: e02249-14.
 22. Lee JW, Park S, Takahashi Y, Wang HG. The association of AMPK with ULK1 regulates autophagy. *PLoS One* 2010;5:e15394.
 23. Jin J, Iakova P, Jiang Y, Medrano EE, Timchenko NA. The reduction of SIRT1 in livers of old mice leads to impaired body homeostasis and to inhibition of liver proliferation. *Hepatology* 2011;54:989-98.
 24. Maruyama N, Ishigami A, Kondo Y. Pathophysiological significance of senescence marker protein-30. *Geriatr Gerontol Int* 2010;10 Suppl 1:S88-98.
 25. Ermolaeva MA, Schumacher B. Insights from the worm: the *C. elegans* model for innate immunity. *Semin Immunol* 2014;26:303-9.
 26. Cinar HN, Kothary M, Datta AR, Tall BD, Sprando R, Bilecen K, Yildiz F, McCardell B. *Vibrio cholerae* hemolysin is required for lethality, developmental delay, and intestinal vacuolation in *Caenorhabditis elegans*. *PLoS One* 2010;5:e11558.
 27. Sahu SN, Lewis J, Patel I, Bozdag S, Lee JH, LeClerc JE, Cinar HN. Genomic analysis of immune response against *Vibrio cholerae* hemolysin in *Caenorhabditis elegans*. *PLoS One* 2012;7:e38200.
 28. Fujii H, Yokozawa T, Kim YA, Tohda C, Nonaka G. Protective effect of grape seed polyphenols against high glucose-induced oxidative stress. *Biosci Biotechnol Biochem* 2006;70:2104-11.
 29. Sakurai T, Nishioka H, Fujii H, Nakano N, Kizaki T, Radak Z, Izawa T, Haga S, Ohno H. Antioxidative effects of a new lychee fruit-derived polyphenol mixture, oligonol, converted into a low-molecular form in adipocytes. *Biosci Biotechnol Biochem* 2008;72:463-76.
 30. Fujii H, Nishioka H, Wakame K, Magnuson BA, Roberts A. Acute, subchronic and genotoxicity studies conducted with Oligonol, an oligomerized polyphenol formulated from lychee and green tea extracts. *Food Chem Toxicol* 2008;46:3553-62.
 31. Salminen A, Ojala J, Kaarniranta K, Kauppinen A. Mitochondrial dysfunction and oxidative stress activate inflammasomes: impact on the aging process and age-related diseases. *Cell Mol Life Sci* 2012;69:2999-3013.
 32. Sena LA, Chandel NS. Physiological roles of mitochondrial reactive oxygen species. *Mol Cell* 2012;48:158-67.
 33. Li X, Fang P, Mai J, Choi ET, Wang H, Yang XF. Targeting mitochondrial reactive oxygen species as novel therapy for inflammatory diseases and cancers. *J Hematol Oncol* 2013;6:19.
 34. West AP, Brodsky IE, Rahner C, Woo DK, Erdjument-Bromage H, Tempst P, Walsh MC, Choi Y, Shadel GS, Ghosh S. TLR signalling augments macrophage bactericidal activity through mitochondrial ROS. *Nature* 2011;472:476-80.
 35. Rutanen J, Yaluri N, Modi S, Pihlajamäki J, Vanttinen M, Ikonen P, Kainulainen S, Yamamoto H, Lagouge M, Sinclair DA, Elliott P, Westphal C, Auwerx J, Laakso M. SIRT1 mRNA expression may be associated with energy expenditure and insulin sensitivity. *Diabetes* 2010;59:829-35.
 36. Agarwal B, Baur JA. Resveratrol and life extension. *Ann N Y Acad Sci* 2011;1215:138-43.
 37. Park JY, Kim Y, Im JA, You S, Lee H. Inhibition of Adipogenesis by Oligonol through Akt-mTOR Inhibition in 3T3-L1 Adipocytes. *Evid Based Complement Alternat Med* 2014; 2014:895272.
 38. Park CH, Yokozawa T, Noh JS. Oligonol, a low-molecular-weight polyphenol derived from lychee fruit, attenuates diabetes-induced renal damage through the advanced glycation end product-related pathway in db/db mice. *J Nutr* 2014;144:1150-7.
 39. Fulco M, Sartorelli V. Comparing and contrasting the roles of AMPK and SIRT1 in metabolic tissues. *Cell Cycle* 2008;7:3669-79.
 40. Cantó C, Gerhart-Hines Z, Feige JN, Lagouge M, Noriega L, Milne JC, Elliott PJ, Puigserver P, Auwerx J. AMPK regulates energy expenditure by modulating NAD⁺ metabolism and SIRT1 activity. *Nature* 2009;458:1056-60.